WIAS-HITNIHS: A SOFTWARE TOOL FOR SIMULATION IN SUBLIMATION GROWTH OF SIC SINGLE CRYSTALS: APPLICATIONS AND METHODS. *

JÜRGEN GEISER †, OLAF KLEIN ‡, AND PETER PHILIP §

Abstract. The numerous technical applications in electronic and optoelectronic devices, such as lasers, diodes, and sensors demand high-quality silicon carbide (SiC) bulk single crystal for industrial applications. We consider a SiC crystal growth process by physical vapor transport (PVT), called modified Lely method. We deal with a model for the thermal processes within the growth apparatus, involving a heat equation with heat sources due to induction heating and nonlocal interface conditions, representing the heat transfer by radiation. The study of the temperature evolution in the apparatus is important for understanding and optimizing the crystal growth process. We present results of some numerical simulations of the growth apparatus with respect to grid refinements and discuss numerical errors in the simpler stationary case.

Keywords: numerical methods, heat equation, radiation, crystal growth process, numerical simulations, stationary case.

1. Introduction and mathematical model. The motivation for this study comes from the technical demand to simulate a crystal growth apparatus for SiC single crystals. The single crystals are used as a high-valued and expensive material for optoelectronics and electronics, cf. [8]. The silicon carbide (SiC) bulk single crystal are produced by a growth process through physical vapor transport (PVT), called modified Lely-method. The modeling for the thermal processes within the growth apparatus is done in [4] and [10]. The underlying equations of the model are given as follows:

a.) In this work, we assume that the temperature evolution inside the gas region $\Omega_{\rm g}$ can be approximated by considering the gas as pure argon. The reduced heat equation is

$$\rho_{\rm g}\partial_t U_{\rm g} \; - \; \nabla\cdot(\kappa_{\rm g}\nabla T) = 0, \tag{1.1}$$

$$U_{\rm g} = z_{\rm Ar}\, R_{\rm Ar}\, T, \tag{1.2}$$

where T is the temperature, t is the time, and $U_{\rm g}$ is the internal energy of the argon gas. The parameters are given as $\rho_{\rm g}$ being the density of the argon gas, $\kappa_{\rm g}$ being the thermal conductivity, $z_{\rm Ar}$ being the configuration number, and $R_{\rm Ar}$ being the gas constant for argon.

b.) The temperature evolution inside the region of solid materials $\Omega_{\rm s}$, e.g. inside the silicon carbide crystal, silicon carbide powder, graphite, and graphite insulation, is described by the heat equation

$$\rho_{\rm s}\;\partial_t U_{\rm s} \; - \; \nabla\cdot(\kappa_{\rm s}\nabla T) = f, \tag{1.3}$$

$$U_{\rm s} = \int_0^T c_{\rm s}(S)\; dS, \tag{1.4}$$

*This work has been supported by the DFG Research Center "Mathematics for key technologies" (FZT 86) in Berlin

†Weierstrass Institute for Applied Analysis and Stochastics (WIAS), Mohrenstrasse 39, D-10117 Berlin, Germany, E-mail: geiser@wias-berlin.de

‡Weierstrass Institute for Applied Analysis and Stochastics (WIAS), Mohrenstrasse 39, D-10117 Berlin, Germany, E-mail: klein@wias-berlin.de

§Institute for Mathematics and its Applications (IMA), University of Minnesota, 400 Lind Hall, 207 Church Street S.E., Minneapolis, MN 55455-0436, USA, E-mail: philip@ima.umn.edu

where ρ_{s} is the density of the solid material, U_{s} is the internal energy, κ_{s} is the thermal conductivity, and c_{s} is the specific heat.

The equations hold in the domains of the respective materials and are coupled by interface conditions, e.g. requiring the continuity for the temperature and for the normal components of the heat flux on the interfaces between opaque solid materials. On the boundary of the gas domain, i.e. on the interface between the solid material and the gas domain, we consider the interface condition

$$\kappa_{\mathrm{g}}\, \nabla T \cdot \mathbf{n}_{\mathrm{g}} + R - J = \kappa_{\mathrm{s}}\, \nabla T \cdot \mathbf{n}_{\mathrm{g}}, \tag{1.5}$$

where $\mathbf{n}_{\mathrm{g}}$ is the normal vector of the gas domain, R is the radiosity, and J is the irradiosity. The irradiosity is determined by integrating R along the whole boundary of the gas domain, cf. [7]. Moreover, we have

$$R = E + J_{\mathrm{ref}}, \tag{1.6}$$

$$E = \sigma\, \epsilon\, T^4 \quad \text{(Stefan-Boltzmann equation)}, \tag{1.7}$$

$$J_{\mathrm{ref}} = (1 - \epsilon)\, J, \tag{1.8}$$

where E is the radiation, J_{ref} is the reflexed radiation, ϵ is the emissivity, and σ is the Boltzmann radiation constant.

The density of the heat source induced by the induction heating is determined by solving Maxwell's equations. We deal with these equations under the simplifying assumption of an axisymmetric geometry, axisymmetric electromagnetic fields, and a sinusoidal time dependence of the involved electromagnetic quantities, following [12]. The considered system and its derivation can be found in [4], [6], and [10].

In this paper, we focus on the discretization and material properties, which are important for realistic simulations. Our underlying software tool WIAS-HiTNIHS, cf. [10], allows us flexibility in the grid generation and for the material parameters.

In the next section, we describe the used discretization.

2. Discretization. For the discretization of the heat equation (diffusion equation), we apply the implicit Euler method in time and the finite volume method for the space discretization, cf. [2], [4], and [10]. We consider a partition $\mathcal{T} = (\omega_i)_{i \in I}$ of Ω such that, for $m \in \{\mathrm{s}, \mathrm{g}\}$ (with s solid, g gas) and $i \in I$, $\omega_{m,i} := \omega_i \cap \Omega_m$ defines either a void subset or a nonvoid, connected, and open polyhedral subset of Ω. By integrating the corresponding heat equation (1.1) or (1.3) over $\omega_{m,i}$, we derive the following nonlinear equations for the temperature variables,

$$\begin{aligned} &\rho_m \int_{\omega_{m,i}} (U_m(T^{n+1}) - U_m(T^n))\, r\, dx \\ &\quad -\Delta t^{n+1} \int_{\partial\omega_{m,i}} \kappa_m(T^{n+1})\, \nabla T^{n+1} \cdot \mathbf{n}_{\omega_{m,i}}\, r\, ds \;=\; \Delta t^{n+1} \int_{\omega_{m,i}} f_m\, r\, dx, \end{aligned} \tag{2.1}$$

where the time interval is $\Delta t^{n+1} = t^{n+1} - t^n$. The temperature is given as $T^{n+1} = T(t^{n+1}, x)$, where x represents cylindrical coordinates. For the right-hand sides, we demand $f_{\mathrm{s}} := f \geq 0$ and $f_{\mathrm{g}} = 0$.
More details of the discretization and of dealing with the interface conditions are presented in [3], [4], [5], and [10].

In the next section, the properties of the materials in the crystal growth apparatus are described.

3. Material properties. For the technical realization of the apparatus, we implement the axisymmetric geometry given in [11], which is presented in Fig. 3.1. Furthermore, the properties of the materials are specified in [3], [4], and [9].

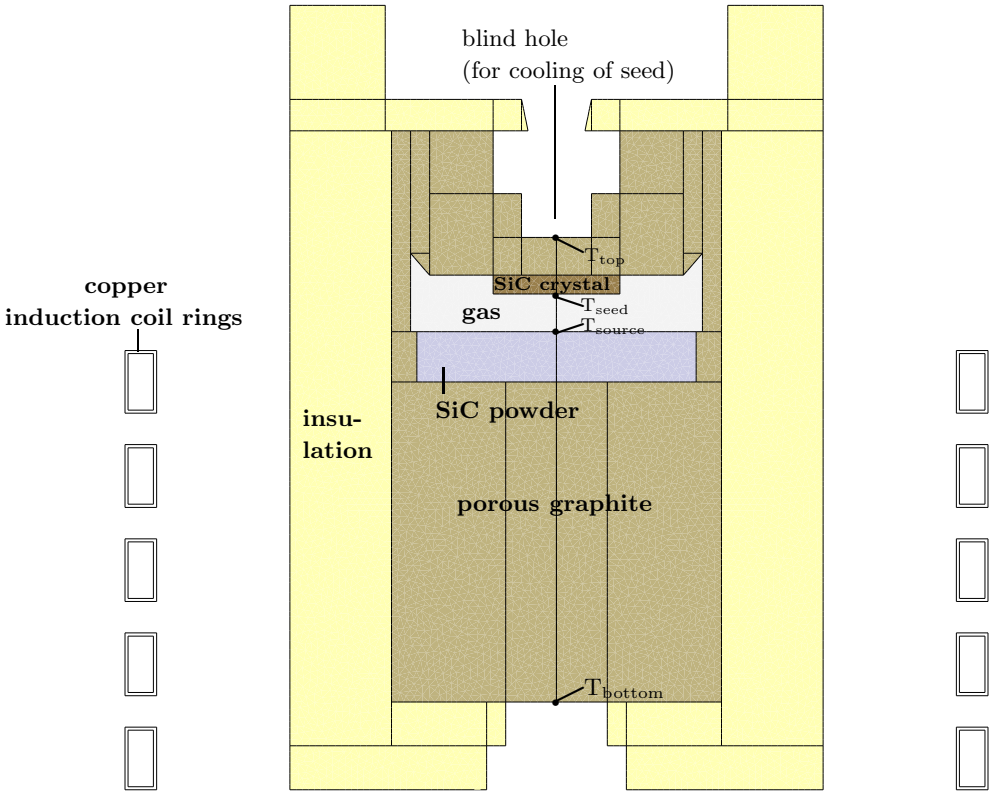

FIG. 3.1. *The growth apparatus' dimensions:* $r_{\min} = 0$, $r_{\max} = 8.4$ cm, $z_{\min} = 0$, $z_{\max} = 25.0$ cm, *the coil rings' dimensions:* $r_{\min} = 4.2$ cm, $r_{\max} = 5.2$ cm, $z_{\min} = 0$, $z_{\max} = 14.0$ cm.

Within the following specific material functions and parameters for the processes, the thermal conductivity κ is given in W/(m K), the electrical conductivity σ_c is given in 1/(Ohm m), the mass density ρ is given in kg/m^3, the specific heat c_{sp} is given in J/(K kg), the temperature T is given in K and the relative gas constant R_{Ar} is given in J/(K kg). Further the emissivity ϵ and relative magnetic permeability μ are given dimensionless.

For the gas phase (argon), we have

$$\kappa_{Ar}(T) = \begin{cases} 1.83914\,10^{-4}\,T^{0.800404} & T \le 500, \\ -7.128738 + 6.610288\,10^{-2}\,T - 2.440839\,10^{-4}\,T^2 & \\ +4.497633\,10^{-7}\,T^3 - 4.132517\,10^{-10}\,T^4 + 1.514463\,10^{-13}\,T^5 & 500 \le T \le 600, \\ 4.1944\,10^{-4}\,T^{0.671118} & 600 \ge T, \end{cases}$$

$\sigma_{c,Ar} = 0.0$, $\rho_{Ar} = 3.73\,10^{-3}$, $\mu_{Ar} = 1.0$, $z_{Ar} = 3/2$, $R_{Ar} = 2.081308\,10^{-2}$.

For graphite felt insulation, we have

$$\kappa_{Ins}(T) = \begin{cases} 8.175\,10^{-2} + 2.485\,10^{-4}\,T & T \le 1473, \\ -1.1902\,10^2 + 0.346838\,T - 3.9971\,10^{-4}\,T^2 + 2.2830\,10^{-7}\,T^3 & \\ -6.46047\,10^{-11}\,T^4 + 7.2549\,10^{-15}\,T^5 & 1473 \le T \le 1873, \\ -0.7447 + 7.5\,10^{-4}\,T & 1873 \ge T, \end{cases}$$

$\epsilon_{\rm Ins} = 0.2$, $\sigma_{c,\rm Ins}(T) = 2.45\ 10^2 + 9.82\ 10^{-2}\ T$, $\rho_{\rm Ins} = 170.00$, $\mu_{\rm Ins} = 1.00$,
$c_{\rm sp,Ins} = 2100.00$.

For the graphite, we have
$\kappa_{\rm Graphite}(T) = 37.715\ \exp(-1.96\ 10^{-4}\ T)$,

$$\epsilon_{\rm Graphite}(T) = \begin{cases} 0.67 & T \le 1200, \\ 3.752 - 7.436\ 10^{-3}\ T + 6.4163\ 10^{-6}\ T^2 & \\ \quad -2.3366\ 10^{-9}\ T^3 - 3.0833\ 10^{-13}\ T^4 & 1200 \le T \le 2200, \\ 0.79 & 2200 \ge T, \end{cases}$$

$\sigma_{\rm c,Graphite} = 10^4$, $\rho_{\rm Graphite} = 1750.0$, $\mu_{\rm Graphite} = 1.0$,
$c_{\rm sp,Graphite}(T) = 1/(4.411\ 10^2\ T^{-2.306} + 7.97\ 10^{-4}\ T^{-0.0665})$.

For the SiC crystal, we have
$\kappa_{\rm SiC\text{-}C}(T) = \exp(9.892 + (2.498\ 10^2)/T - 0.844\ \ln(T))$,
$\epsilon_{\rm SiC\text{-}C} = 0.85$, $\sigma_{\rm c,SiC\text{-}C} = 10^5$, $\rho_{\rm SiC\text{-}C} = 3140.0$, $\mu_{\rm SiC\text{-}C} = 1.0$,
$c_{\rm sp,SiC\text{-}C}(T) = 1/(3.91\ 10^4\ T^{-3.173} + 1.835\ 10^{-3}\ T^{-0.117})$.

For the SiC powder, we have
$\kappa_{\rm SiC\text{-}P}(T) = 1.452\ 10^{-2} + 5.47\ 10^{-12}\ T^3$,
$\epsilon_{\rm SiC\text{-}P} = 0.85$, $\sigma_{\rm c,SiC\text{-}P} = 100.0$, $\rho_{\rm SiC\text{-}P} = 1700.0$, $\mu_{\rm SiC\text{-}P} = 1.0$, $c_{\rm sp,SiC\text{-}P} = 1000.0$.

The functions are programmed in our flexible software package WIAS-HiTNIHS. In the next section, we present results of our numerical experiments.

4. Numerical experiments. For the numerical results, we apply the parameter functions in Section 3. We consider the geometry shown in Fig. 3.1, using a constant total input power of 10 kW, cf. [11]. The numerical experiments are performed using the software WIAS-HiTNIHS, cf. [10], based on the software package *pdelib*, cf. [1], which uses the sparse matrix solver *PARDISO*, cf. [13]. We compute the coupled system consisting of the heat equations and Maxwell's equations. For the growth process, the temperature difference $T_{\rm ss} = T(r_{\rm source}, z_{\rm source}) - T(r_{\rm seed}, z_{\rm seed})$ (with the coordinates $(r_{\rm source}, z_{\rm source}) = (0, 0.143)$ and $(r_{\rm seed}, z_{\rm seed}) = (0, 0.158)$, corresponding to the points $\rm T_{source}$ and $\rm T_{seed}$ in Fig. 3.1) is crucial. On the other hand, in the physical growth experiments, usually only the temperatures $T(r_{\rm bottom}, z_{\rm bottom})$ and $T(r_{\rm top}, z_{\rm top})$ (with the coordinates $(r_{\rm bottom}, z_{\rm bottom}) = (0, 0.028)$ and $(r_{\rm top}, z_{\rm top}) = (0, 0.173)$, corresponding to the points $\rm T_{bottom}$ and $\rm T_{top}$ in Fig. 3.1) are measurable and their difference $T_{\rm bt} = T(r_{\rm bottom}, z_{\rm bottom}) - T(r_{\rm top}, z_{\rm top})$ is often used as an indicator for $T_{\rm ss}$. In Fig. 4.1, we present the temperature differences $T_{\rm ss}$ and $T_{\rm bt}$. As a result of our computations, the temperature difference $T_{\rm bt}$ can only restrictively be used as an indicator for the temperature difference $T_{\rm ss}$, cf. the discussions in [3] and [7].

The further computations are based on the stationary case, dealing with Equation (1.1) by discarding the terms with a time derivative. For this case, the results are virtually equal to the one in the transient case with $t > 15000$ sec. For the stationary results, we focus on the error analysis for the space dimension by applying the grid refinement. The solutions for the heat equation are computed at the points $T(r_{\rm bottom}, z_{\rm bottom})$ and $T(r_{\rm top}, z_{\rm top})$ for successive grids. For the error analysis, we apply the following error differences

$$\epsilon_{\rm abs} = |\tilde{T}_{j+1}(r, z) - \tilde{T}_j(r, z)|, \tag{4.1}$$

where $\tilde{T}_j(r, z)$ and $\tilde{T}_{j+1}(r, z)$ are solutions evaluated at the point (r, z) which have been computed using the grids j and $j + 1$ respectively. The elements of the grid

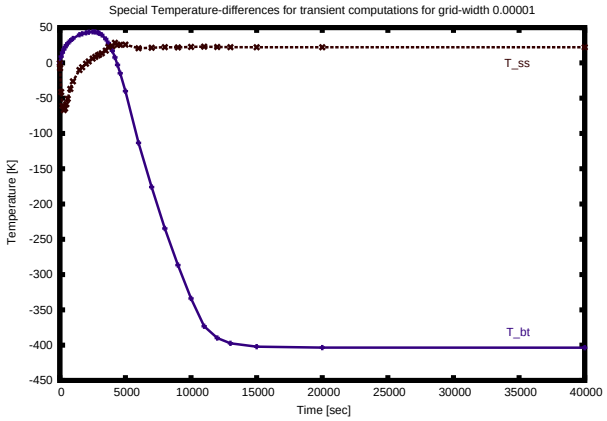

FIG. 4.1. *Transient results for the temperature differences T_{bt} and T_{ss}.*

$j+1$ are approximately 1/4 of the elements of the grid j. The results are presented in Table 4.1.

Grid		Grid Point $(0, 0.028)$ ($\mathrm{T_{bottom}}$)		Grid Point $(0, 0.173)$ ($\mathrm{T_{top}}$)	
Level	Number of Nodes	Solution T [K]	Absolute Difference T [K]	Solution T [K]	Absolute Difference T [K]
0	1532	2408.11		2813.29	
1	23017	2409.78	1.67	2812.78	1.01
2	91290	2410.35	0.57	2811.79	0.49
3	364225	2410.46	0.11	2811.60	0.19

TABLE 4.1
Computations on different grids for the errors analysis with absolute differences, cf. (4.1).

The result of the refinement indicates the reduction of the absolute difference as it is demanded for the convergence of the discretization method. The method is stabilized in the presented refinement by reducing the differences.

In Fig. 4.2, the temperature field is presented for the stationary case. The temperature increases from the bottom to the middle of the graphite pot, and decreases from the middle to the top of the graphite pot.

In the next section, we present the conclusion of our simulations.

5. Conclusion. We have presented a model for the heat transport inside a technical apparatus for crystal growth of SiC single crystals. We introduce the heat equation and the radiation of the apparatus and the coupled situation of the different materials. The equations are discretised by the finite volume method and the complex material functions are embedded in this method. Transient and stationary results are presented leading to some information about the processes within the technical apparatus. We present numerical results for the stationary case to support the accuracy of our solutions. In our future work, we concentrate on further implementations and numerical methods for a crystal growth model.

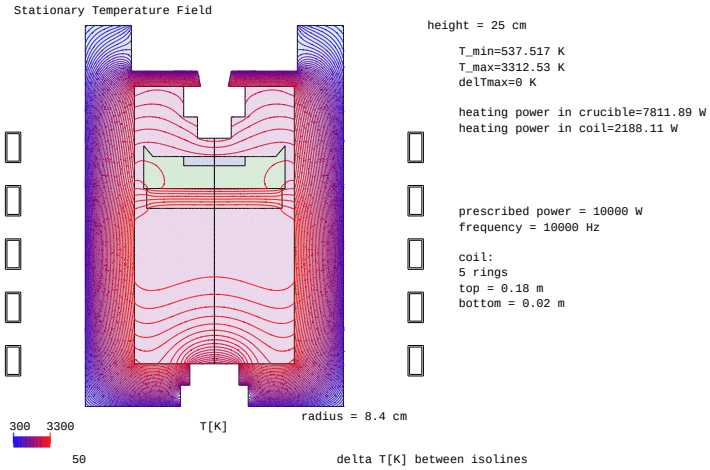

FIG. 4.2. *Temperature field for the apparatus simulated for the stationary case with* 23017 *nodes.*

REFERENCES

[1] J. Fuhrmann, Th. Koprucki and H. Langmach. *pdelib : An open modular tool box for the numerical solution of partial differential equations. Design patterns.* In W. Hackbusch and G. Wittum;, editors, Proceeding of the 14th GAMM Seminar on Concepts of Numerical Software, January 23 - 25, 1998. Kiel, 2001.

[2] J. Geiser. *R^3T : Radioactive-Retardation-Reaction-Transport-Program for the Simulation of radioactive waste disposals.* Technical report, Institute for scientific computation, Texas A&M University, College Station, April 2004.

[3] O. Klein, P. Philip. *Transient temperature phenomena during sublimation growth of silicon carbide single crystals.* Journal of Crystal Growth, 249, 514-522, 2003.

[4] O. Klein and P. Philip. *Transient numerical investigation of induction heating during sublimation growth of silicon carbide single crystals.* J. Crystal Growth, 247, no. 1-2, 219–235, 2003.

[5] O. Klein and P. Philip. *Transient conductive-radiative heat transfer: Discrete existence and uniqueness for a finite volume scheme.* Preprint No. 871, Weierstrass-Institute for Applied Analysis and Stochastics, Berlin 2003.

[6] O. Klein and P. Philip. *Correct voltage distribution for axisymmetric sinusoidal modeling of induction heating with prescribed current, voltage, or power.* IEEE transactions on Magnetics, 38, no. 3, pp. 1519-1523, 2002.

[7] O. Klein, P. Philip and J. Sprekels. *Modeling and simulation of sublimation growth of SiC bulk single crystals.* Interfaces and Free Boundaries, 6, 295-314, 2004.

[8] St.G. Müller, R.C. Glass, H.M. Hobgood, V.F. Tsvetkov, M. Brady, D. Henshall, D. Malta, R. Singh, J. Palmour and C.H. Carter Jr. *Progress in the industrial production of SiC substrate for semiconductor devices.* Mater. Sci. Eng. ,B 80 , no. 1-3, 327–331, 2002.

[9] O. Nilsson, H. Mehling, R. Horn, J. Fricke, R. Hofmann, S.G. Müller, R. Eckstein, and D. Hofmann. *Determination of the thermal diffusivity and conductivity of monocrystalline silicon carbide (300-2300 K).* High Temp. - High Press., 29, no. 1, 73–80, 1997.

[10] P. Philip. *Transient Numerical Simulation of Sublimation Growth of SiC Bulk Single Crystal. Modeling, Finite Volume Method, Results.* Report No. 22, Weierstrass-Institute for Applied Analysis and Stochastics, Berlin, 2003.

[11] M. Pons, M. Anikin, K. Chourou, J. Dedulle, R. Madar, E. Blanquet, A. Pisch, C. Bernard, P. Grosse, C. Faure, G. Basset, and Y. Grange. *State of the art in the modeling of SiC sublimation growth.* Mater. Sci. Eng. B, **61**–**62**, 18–28, 1999.

[12] J. Rappaz and M. Swierkosz. *Modelling in numerical simulation of electromagnetic heating.* Modelling and optimization of distributed parameter systems, New-York. Chapmann & Hall, 313–320, 1996.

[13] O. Schenk, K. Gärtner. *Solving unsymmetric sparse systems of linear equations with PARDISO* J. Future Generation Computer Systems, **20**, no. 3, 475–487, 2004.